Jurnal Tribologi 39 (2023) 51-68

MYTRIBOS Malaysian Tribology Society

Jurnal Tribologi

Website : jurnaltribologi.mytribos.org e-issn: 2289-7232

Enhancing physical, mechanical, tribological and contact characteristics of water-based lubrication using ceramic nanomaterials MgO and SiC for metal-to-metal sliding interfaces

Leong Ming Rui [1], Mohd Hafis Sulaiman [1*], Muhammad Ashman Hakimi Azizan Ashman [1], Muhammad Shuhaimi Ibrahim [1], Mohd Ridzuan Mohd Jamir [2]

[1] Department of Mechanical and Manufacturing Engineering, Faculty of Engineering, Universiti Putra Malaysia, MALAYSIA.
[2] Faculty of Mechanical Engineering and Technology, Universiti Malaysia Perlis, MALAYSIA.
[*]Corresponding author: hafissulaiman@upm.edu.my

KEYWORDS

Ceramic-based nanoparticles
Magnesium oxide
Silica carbide
Water-based lubricants
Nanolubricants
Nanoadditives
Tribological characteristics
Lubrication mechanism

ABSTRACT

Water-based lubricants offer cost-effective benefits and are safer for both the environment and human personnel compared to oil-based lubricants. In this study, ceramic-based nanoparticles, namely MgO and SiC, were investigated as nanoadditives to enhance the performance of water-based lubrication. The methodology involved formulating the nanoparticles in water-based lubricants and characterizing the sedimentation, physical, mechanical, thermal and tribological properties. The results demonstrated that the dispersion stability of the lubricants improved when mixed with Glycerol and Polyvinylpyrrolidone. Both MgO and SiC nanoparticles exhibited enhancements in viscosity, friction, wear, and thermal properties. This improvement was further validated through FESEM-EDS analysis, which revealed a reduction in friction and wear owing to the ball-bearing effect and the formation of a protective film. Moreover, the study highlighted the deposition of nanoparticles on the contact surfaces, which not only facilitated the mending effect but also played a significant role in reducing surface roughness by acting as a polishing agent.

Received 4 July 2023; received in revised form 5 August 2023; accepted 22 October 2023.
To cite this article: Rui et al., (2023). Enhancing physical, mechanical, tribological and contact characteristics of water-based lubrication using ceramic nanomaterials MgO and SiC for metal-to-metal sliding interfaces. Jurnal Tribologi 39, pp.51-68.

1.0 INTRODUCTION

According to research by Holmberg and Erdemir (2019), approximately 20% of the energy consumption in the world are caused by friction, and an average of 30% of these energy losses can be reduced by using the latest technology of materials, lubricants, and tribo-system design. Among these, lubricants, namely neat oils and oil-in-water emulsions, are commonly used and have shown positive results to enhance tribological performance (Morshed et al., 2021). However, the traditional oil-based lubricants, ie. derived from petroleum or mineral oil sources, used often have environmental issues, such as difficulty of post-cleaning and disposal due to the non-biodegradable nature of oil (Zhou et al., 2022), inclusion of non-biodegradable additives (Zahedi et al., 2019), and potential depletion of the fossil fuel reserve within the next 50 years (Rahman et al., 2021).

To counter the negative impact from the use of oil-based lubricants, one of the alternatives, Water-Based Lubricants (WBLs) have shown promising results as an eco-friendly lubricant and demonstrated great potential in engineering applications, such as hydropower, machining, metal forming, etc. (Morshed et al., 2021). Furthermore, WBLs exhibit various benefits, such as low cost, excellent thermal conductivity and cooling capacity, high fluidity besides its environment friendliness (Wang et al., 2021). Unfortunately, the WBLs have poor tribological properties since it has poor performance in friction reduction, low viscosity, and corrosive properties, which makes it unsuitable for many tribological applications (Rahman et al., 2021). To overcome the disadvantages of water-based lubricants, nanoparticles can be incorporated to improve their properties and performance, which merges the excellent lubricity of nanoadditives and high cooling capacity of water (Morshed et al., 2021). However, determining the ideal nanoparticles for water-based lubricants remains a challenge, and more understanding of the mechanisms and effects of nanoadditives on the lubricants is required (Aikin, 2023).

Nanoparticles are particles with size of less than 100 nm in minimum one dimension out of the three-dimensional space (Han et al., 2022). With the small size, the nanoparticles can easily enter the small space between asperities and efficiently exhibit their excellent tribological properties (Abe et al., 2020). They can be categorized according to their shape, as in sphere-, sheet-, onion- and nanotube-like nanoparticles. Depending on the shape, the nanoparticles may have different lubrication mechanisms, such as rolling effect, mending effect, polishing effect and protective film formation. The concentration of nanoparticles in water-based lubricant is an important factor that can significantly impact the performance and properties of the lubricant. Recent findings on these SiC and MgO ceramic-based nanoparticles in synthetic oil-based lubricants at optimum concentration of 0.3 wt%. were found through pin-on-disk test to be able to reduce coefficient of friction (COF) by 66 % and 25 % respectively (Ahamed et al., 2020). Ding et al. (2018) performed reciprocating friction test on different weightage of Calcium Carbonate ($CaCO_3$) nanoparticles under different load, in which it has been determined that the 3 wt% $CaCO_3$ nanolubricant can reduce the COF by 17.65 %, relative to pure hydraulic oil at 60 N load. Ammarullah et al. (2023) also studied the use of ceramic-based materials in hard-on-hard bearing in which proven that ceramic-based materials reduce the maximum deformation and running-in linear and volumetric wear compared to other materials.

The physical, mechanical and tribological properties of WBLs can be enhanced with ceramic-based nanoparticles. Ceramic-based nanoparticles are considered more biocompatible and environmentally friendly than certain other nanoparticle types, particularly metallic nanoparticles. Ceramic-based nanoparticles are composed of inorganic materials from sustainable sources that are commonly found in nature. These ceramic materials can undergo

degradation processes over time through natural mechanisms such as dissolution or surface reactions, leading to the breakdown of the nanoparticles into smaller, less harmful components. Therefore, the main aim of the study is to formulate WBLs by incorporating the ceramic-based nanoparticles, which are MgO and SiC, with deionized (DI) water for comparison. This involved an investigation into the sedimentation, physical, mechanical, thermal and tribological properties of the formulated WBLs. The physico-chemical and mechanical properties of the WBLs, including dispersion stability and viscosity, were investigated using sedimentation analysis and rheometer respectively. The friction and wear characteristics were analyzed in a customized cylindrical block-on-ring tribology test according to the ASTM G77 standard. FESEM-EDS analysis was conducted after the tribology test to understand the contact mechanism of the formulated WBLs on the metal-to-metal sliding interfaces.

2.0 MATERIALS AND METHODOLOGY

2.1 Formulation of Test Lubricants

The materials for preparing water-based nanolubricants were the nanoparticles, base liquid, which was DI water, and surfactants to improve the dispersion stability of nanoparticles. The surfactant used was Polyvinylpyrrolidone (PVP) since it has shown better effectiveness and wider use relative to other surfactants (He et al., 2017). Additionally, glycerol was added to improve the viscosity of the lubricants, which beneficial to improve the load carrying capacity of the base lubricant (Zhou et al., 2022). The ceramic-based nanoparticles used for this study were MgO and SiC. In this study, both MgO and SiC have a purity of 99% and particle sizes ranging from 20 to 30 nm for MgO and 20 to 40 nm for SiC. The range size of nanoparticles were kept around the same range to avoid difference in the tribological performance as stated by Paijan et al. (2023). The MgO was purchased from Jiangsu XFNano Materials Tech Co., while the SiC was supplied by Xi'an LY Health Technology Co. The MgO was selected because it has high hardness and melting point, high solubility and low density (Singh et al., 2021). Meanwhile, the SiC was chosen since it has good self-lubrication, high hardness, wear resistance, and thermal conductivity (Zhang et al., 2016). Both ceramic-based nanoparticles MgO and SiC offered significant improvements in lubrication due the facts that both MgO and SiC may activate different lubrication mechanisms such as rolling, mending, polishing and protective film formation effects between metal-to-metal sliding interfaces (Morshed et al., 2021; Han et al., 2022).

The WBLs were prepared using two step method similar to Zhou et al. (2022) as presented in Figure 1, with the formulation summarized in Table 1. The DI water was mixed with glycerol using magnetic stirrer. Then, PVP was added drop by drop into the solution with magnetic stirring running at 1,200 rev/min. Then, the ceramic-based nanoparticles MgO or SiC was gradually added into the solution and mixed with overhead stirrer at 1,200 rpm for 30 minutes and until no obvious agglomeration was formed in the WBLs. The remaining agglomeration was then removed by 120 W bath ultrasonication for another 30 min. To further improve the dispersion stability of the ceramic-based nanoparticles SiC in the WBLs, the pH of the WBL was adjusted to pH 10 using sodium hydroxide solution (Akilu et al., 2016).

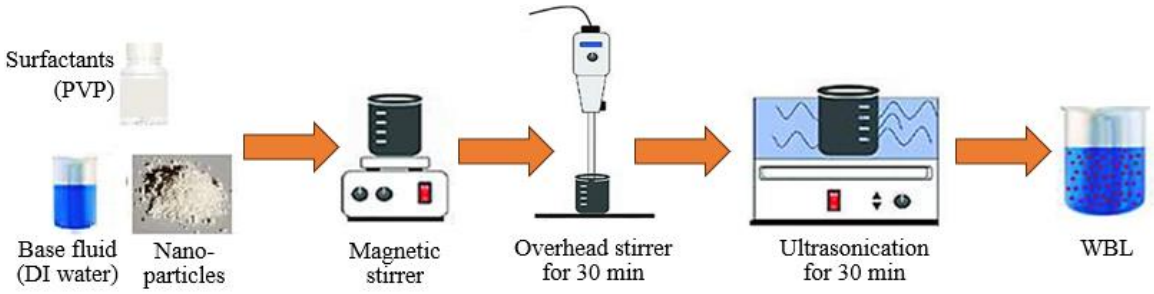

Figure 1: Preparation to achieve better dispersion stability of water-based nanolubricants.

Table 1: Formulation of water-based nanolubricants.

Test Lubricants	Content
DI Water	DI water
MgO	0.3 wt% MgO nanoparticles + DI water + 2.0 wt% glycerol + 0.05 wt% PVP (Ahamed et al., 2020; Qamar et al., 2022)
SiC	0.3 wt% SiC nanoparticles + DI water + 2.0 wt% glycerol + 0.05 wt% PVP (Ahamed et al., 2020; Chen et al., 2017)

2.2 Physical and Mechanical Properties Characterization

Sedimentation analysis method was used to determine the dispersion stability of the water-based nanolubricants for its simplicity and low cost. After each nanolubricant was prepared, a sample was collected immediately for analysis. The samples were photographed every 24 hours for 3 days. In addition, the morphology of the nanoparticles in WBLs was observed using JEOL JEM 2100F Field Emission Transmission Electron Microscope (FETEM).

As for rheological behaviour of WBLs, a viscosity test was conducted using the Anton Paar MCR 72 rheometer (Anton Paar, Graz, Austria) in accordance with ASTM D445 with a cone plate geometry of 1° cone angle and 50-mm diameter, in which the viscosity was measured at a shear rate 3,000 s^{-1} from 30 °C to 50 °C by using a Peltier plate. The temperature range for conducting the viscosity test was determined by analyzing the results of the tribological test. It was observed that the temperature profiles remained below 50 °C.

2.3 Tribological Characterization

The tribological performance of the WBLs were assessed using Block-on-Ring (BOR) test (Figure 2) (Seidel et al., 2019) following the standard ASTM G77-98 as detailed in our previous work (Sharuddin et al., 2023). The cylindrical block and ring materials used in each test were made of AISI 52100 bearing steel, in which the properties are listed in Table 2.

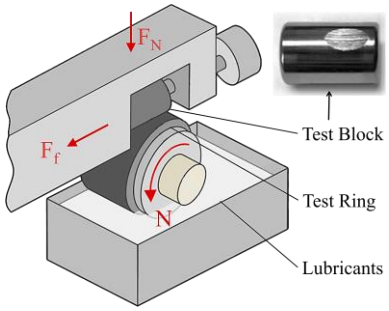

Parameters	Details
Block	*Ø*14 mm x *L*14 mm, 67 HRC, *Ra*=0.0363 µm, *Rq*=0.0455 µm
Ring	*Ø*40 mm x *W*12 mm, 68.1 HRC, *Ra*=0.6453 µm, *Rq*=0.8317 µm
Normal Load F_N	490.5 N (equivalent to Hertzian stress of 205.303 MPa)
Speed *N*	490 rev/min
Temperature *T*	31 °C (room temperature)

Figure 2: Schematic diagram of block-on-ring test (left) and test parameters (right).

Table 2: General properties of the materials of the block and ring (MatWeb, n.d.)

Material properties	AISI 52100 bearing steel
Density ρ	7.81 g/cm^3
Vickers Hardness	690 HV
Elastic modulus *E*	210 GPa
Yield strength σ_Y	1,800 MPa
Ultimate strength σ_U	2,400 MPa
Chemical composition	Fe 96.5%, Cr 1.6%, C 1.1%, Mn 0.45%, Si 0.3%, P 0.025%, S 0.025%

To perform the tribology test, the WBL to be tested was mixed for 15 minutes prior to each test. The block and ring surfaces were additionally cleaned using acetone to remove oil and dirt residues, ensuring a thorough cleaning of the surfaces. The block and ring were then weighed and were handled carefully with lint-free gloves to avoid contamination or addition of weight. Then, the tribometer was set up and started with the test parameters as listed in Figure 2. During the test, the contact load, speed, current and temperature were measured and recorded. The test was repeated from the first step by using a new block for different WBLs.

After the tribology test, the dimensions and surface profile of the worn surfaces for different WBLs were determined by using a microscope Dino-Lite AM4113. Furthermore, the distribution of nanoparticles and type of wear on the worn surface after each tribology test were observed using FESEM and EDX mapping to determine the lubrication mechanism. The equipment used was the FEI Nova NanoSEM 230 Field Emission Scanning Electron Microscope (FESEM) equipped with Oxford Instruments Energy Dispersive X-ray (EDX). Figure 3 below summarizes the methodology of wear analysis using both optical microscope and FESEM-EDX (Seidel et al., 2019).

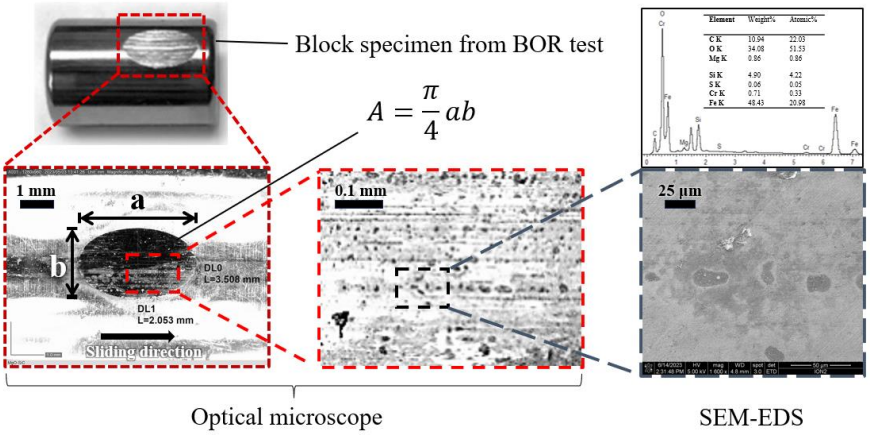

Figure 3: Methodology of wear analysis using optical microscope and FESEM-EDX.

2.4 Film Thickness and Lubrication Regime Determination

Dimensionless film thickness λ can help predict the lubrication regime, where $\lambda > 3.0$ represents the hydrodynamic lubrication regime, $1.0 \leq \lambda \leq 3.0$ is the mixed lubrication regime and $\lambda < 1.0$ indicates the boundary lubrication regime. Hence, the dimensionless film thickness λ of the formulated WBLs under different values of Hersey number, $\eta V/F_N$ ("viscosity × rotational speed / normal load") can be estimated using the Dowson-Higginson formula as described in the study conducted by Sidh et al. (2023). The Coefficient of Friction (COF) μ and dimensionless film thickness λ for the block-on-ring test with cross cylinders and point contact can be determined by applying the formula provided in the following description:

$$\mu = \frac{F_f}{F_N} \tag{1}$$

$$G_* = \alpha \times E' \tag{2}$$

$$U_* = \mu_0 \times \frac{u_1 + u_2}{E' \times R_x} \tag{3}$$

$$W_* = \frac{F_N}{E' \times R_x \times L} \tag{4}$$

$$h_{min} = 0.985 \times (U_*)^{0.7} \times (G_*)^{0.6} \times (W_*)^{-0.11} \tag{5}$$

$$\lambda = \frac{h_{min}}{\sqrt{R_{q1}^2 + R_{q2}^2}} \tag{6}$$

where, μ is Coefficient of Friction (COF), G_*, U_*, W_* are dimensionless parameters, α is Pressure viscosity coefficient, μ_0 is absolute viscosity, u is velocity of block and ring, h_{min} is minimum film thickness, and λ is dimensionless film thickness.

3.0 RESULTS AND DISCUSSION

3.1 Morphology of Nanoparticles

The morphology and structure of the nanoparticles in WBLs observed using TEM are shown in Figure 4 (right). From Figure 4 (right), it is observed that the shapes of MgO and SiC nanoparticles are generally irregular with near spherical and hexagonal shape, particularly SiC nanoparticles with a more angular shape. Most of their sizes are approximately 20 – 40 nm. However, Yang et al. (2012) discovered in his research that TEM micrograph does not necessarily reflect the size and dispersion stability of nanoparticles accurately as the sample preparation for TEM often resulted in dried agglomerated nanoparticles.

3.2 Dispersion Stability of Test Lubricants

The dispersion stability can be determined visually through the amount of supernatant. The photographs for sedimentation test are shown in Figure 4. From Figure 4, it is observed that the MgO and SiC nanoparticles remained stable and homogenous in the WBLs throughout the three days. Herein, all WBLs can be considered dispersed.

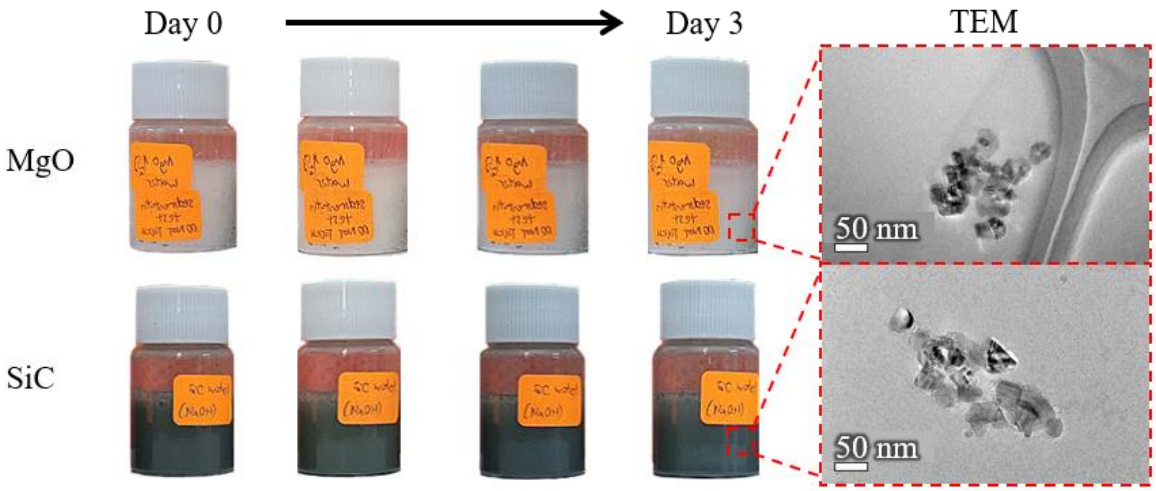

Figure 4: Sedimentation test of WBLs from Day 0 to Day 3 and TEM images of WBLs.

3.3 Viscosity Characteristics of Test Lubricants

The dynamic viscosity of WBLs at different temperatures and at 30 °C were presented in Figure 5. All WBLs have a similar trend of decrease of viscosity with temperature so their rheological behaviour should share similar trend at different temperature. These results agree with the literature and can be explained by how viscosity and particle mobility are inversely proportional with each other, and the mobility of particles increases with temperature. Additionally, the

attraction between the water particles and nanoparticles weakens with an increase in temperature (Arafat et al., 2023). As seen in Figure 5, the dynamic viscosities of WBLs are higher than that of DI water due to the addition of nanoparticles and glycerol. Among the nanolubricants, WBL with SiC has the highest dynamic viscosity (1.004 mPa·s), followed by the WBL with MgO that has the dynamic viscosity of 0.978 mPa·s.

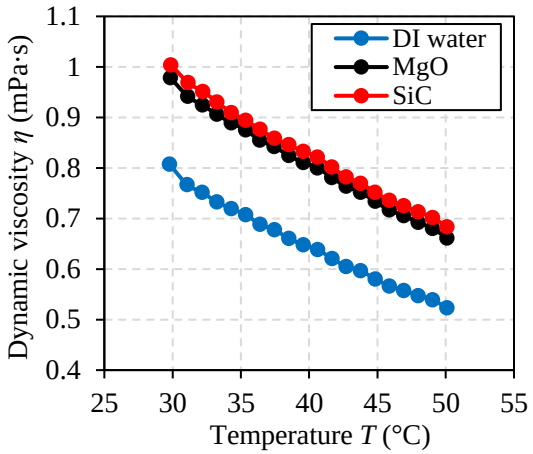

Figure 5: Measurement of dynamic viscosity of WBLs from 30 °C to 50 °C.

3.4 Tribological and Temperature Characteristics

The friction coefficient and temperature against sliding distance of each test lubricant were plotted and presented in Figure 6 and Figure 7. Generally, the lubricants show a high COF and temperature at the early stage, which is known as the running-in period. Afterwards, the COF and temperature slowly decrease to a plateau, which is known as the steady-state period. This trend is commonly observed in various literature, where the higher COF during running-in period is caused by the lack of lubricating layer between the mating surfaces in the early stages of the experiment, leading to severe asperity contact occurred and material removal took place (Sulaiman et al., 2019; Awang et al., 2022). Then, steady-state period begins as the surface becomes smoother, and a lubricating layer may form over time, reducing the COF and making it almost irrelevant to the distance (Hafis et al., 2013; He et al., 2017). Thereby, less heat is generated, and the heat can be quickly removed by the water with high cooling capacity, reducing the temperature.

From both Figure 6 and Figure 7, WBLs generally have lower COF and temperature than water, showing that the nanoparticles generally have improved the friction performance. Among various WBLs, MgO WBL have the lowest average COF (0.317), while SiC WBL have almost similar average COF (0.325). This result revealed MgO nanoparticle was able to improve tribological performance better than SiC nanoparticle, and it was due to their different physical properties and shape features, in which the SiC nanoparticles with irregular and multi-angular shape can plough the surface and the abrasiveness strength of the SiC potentially destroy the lubrication film (Zhang et al., 2016).

According to Figure 7, SiC WBL has the lowest average temperature (35.46 °C) or 31.08 % lower than water, while MgO WBL has the slightly higher average temperature (37.14 °C) than the SiC. Overall, the temperatures for the WBLs are relatively low as the temperature for oil-based

lubricants can easily reach interface temperature that is well above 80°C under high load (Chu et al., 2010; Smazalová et al., 2014; Wu et al., 2018). This demonstrates the high cooling capacity of WBLs, which is mainly due to high heat capacity of water.

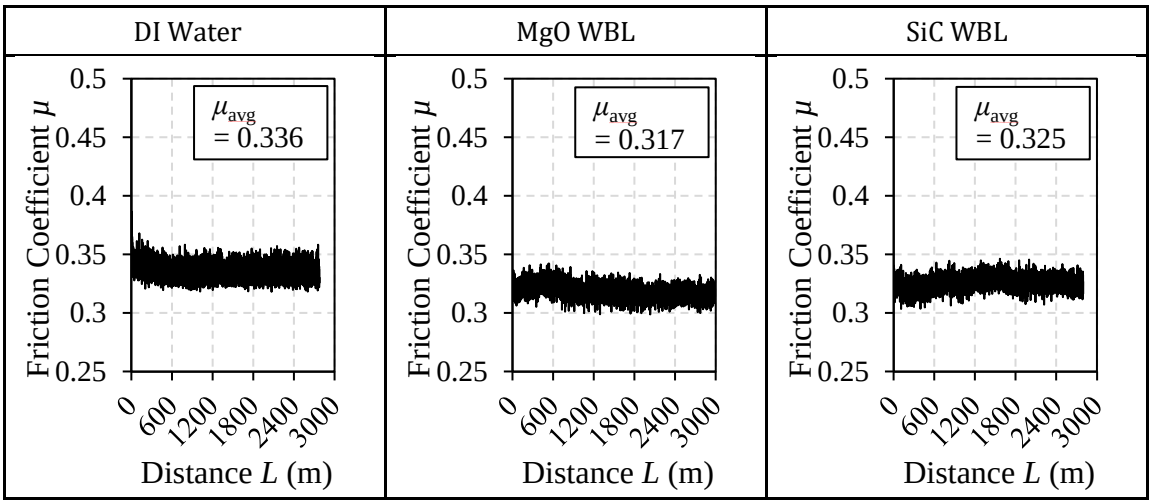

Figure 6: Measurement of friction coefficient μ against sliding distance for different test lubricants.

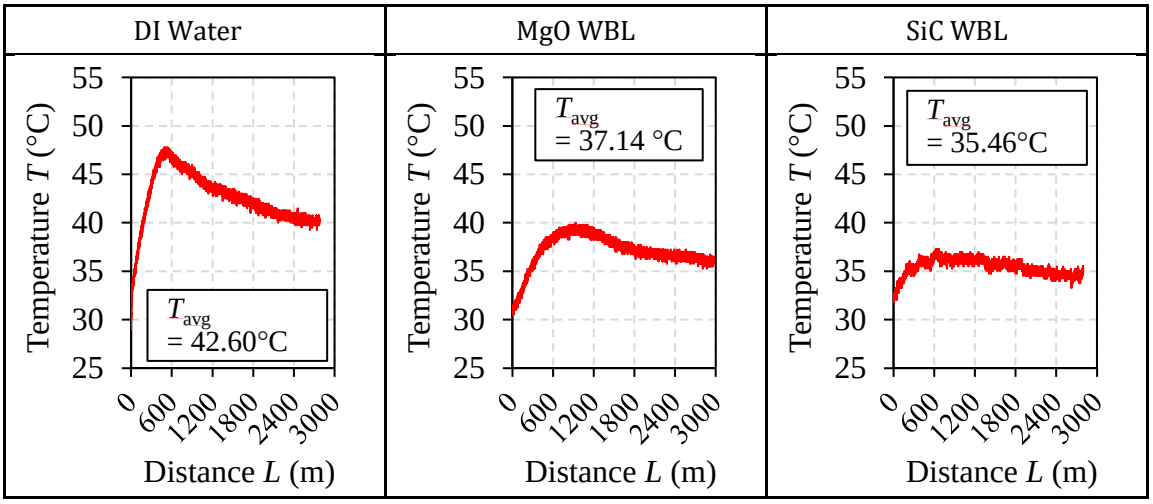

Figure 7: Measurement of temperature T on cylindrical block against sliding distance for different test lubricants.

In general, there is some correlation between average friction coefficient and temperature, which is aligned with the general idea where friction creates heat. The variability may be caused by the thermal properties of the nanoparticles in the WBL, in which some of them may be able to dissipate heat better than others due to their higher thermal conductivity despite the higher friction. For example, the fact that SiC WBL has a higher average friction coefficient but lower average temperature than MgO WBL can be attributed to the higher thermal conductivity of SiC WBL as shown in research by Ahamed et al. (2020). Moreover, this result matches with value of

dynamic viscosity in Figure 5, where it was proved that the decrease of friction coefficient is caused by an increase in the viscosity, creating thicker film and reducing the collision of asperities (Ahamed et al., 2020; He et al., 2017).

3.5 Wear Analysis

The photographs of wear scar of the cylindrical block under different lubricants were studied and observed using Dino-Lite Microscope (see Figure 8), in which larger wear area indicates higher wear rate. Based on Figure 8 MgO WBL have the smallest wear area (2.954 mm^2) and reduce the wear the most (76.69 % relative to water), while the DI water have the largest wear area (9.410 mm^2). The low wear rate caused by MgO WBL was also observed in Figure 9, in which adding the ceramic-based nanoparticles into the WBLs not only increased the viscosity but also reduced wear. In the case of SiC WBL, it may be attributed to the high hardness of the SiC itself (Arafat et al., 2023), which can make it act as abrasive grains. This creates a polishing effect and increases the material removal rate during sliding, forming a larger wear scar with lower friction coefficient (Huang et al., 2019). The nano-sized ceramic-based particle of MgO and SiC observed in TEM imaging (Figure 4) may contributed to low wear rate and higher Brugger value as it is easier for the nanoparticles to enter the small space between pure asperities and separate the tribo-pairs (Abe et al., 2020).

After obtaining the worn area of the different test lubricants, the minimum film thickness and dimensionless film thickness λ can be estimated using Eqn. 1 to 6 and were tabulated in Table 3. From Table 3, the dimensionless film thickness has similar trend on the viscosity of the lubricants because the only parameter that is varied in the formula for dimensionless film thickness is viscosity while the other parameters are or assumed to be constant, in which SiC WBL have the highest dimensionless film thickness (0.362) whereas DI water have the lowest dimensionless film thickness (0.311). The result is similar to other research that work on WBLs, in which the lubrication regime for the WBLs is boundary lubrication regime since the dimensionless film thickness is less than 1 (He et al., 2017; Xie et al., 2018). The WBL worked within the boundary lubrication range meant that the protective film of the WBLs may be unable to form and separate the metal-to-metal sliding surfaces, leading to higher friction, and the occurrence of abrasive and adhesive wear.

DI Water	MgO WBL	SiC WBL
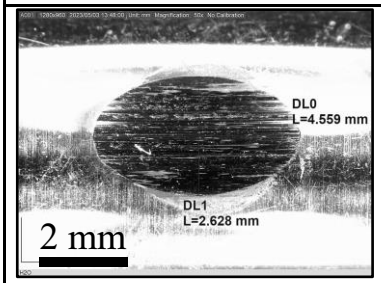	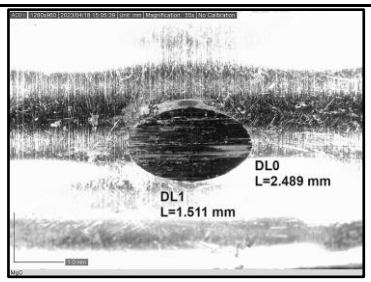	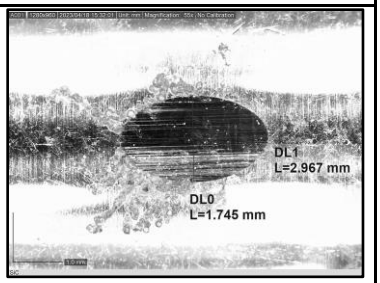
A = 9.410 mm^2	A = 2.954 mm^2	A = 4.066 mm^2

Figure 8: Measurement of worn scar area A for different test lubricants.

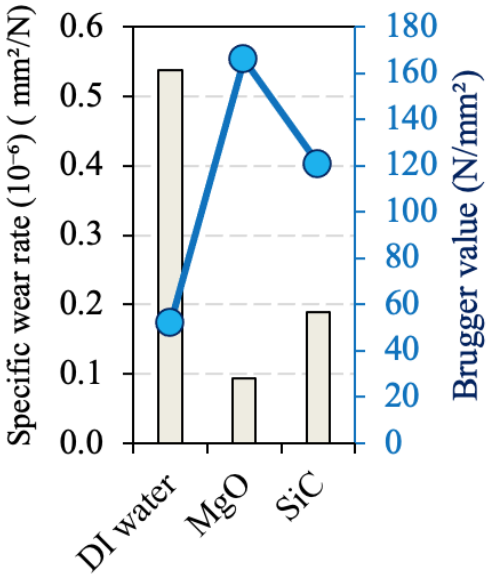

Figure 9: Resulting wear for different test lubricants.

Table 3: Minimum film thickness and dimensionless film thickness of WBLs.

WBLs	**Minimum film thickness h_{min} (µm)**	**Dimensionless film thickness λ**
DI water	0.259	0.311
WBL MgO	0.296	0.356
WBL SiC	0.302	0.362

The worn-out surfaces of the cylindrical blocks were studied and observed using FESEM/EDX for different lubricants as presented in Figure 10. From Figure 10, the wear mechanism for DI water is mostly adhesive wear with some abrasive wear as the wear scar has obvious ploughing grooves with some scratches. Additionally, severe delamination was visible in the FESEM image, showing direct metal-to-metal contact that caused wear debris to be acted as abrasive grains and created the parallel grooves. The rough surface for DI water aligns with the higher friction coefficient obtained earlier in Figure 6 and highest temperature illustrated in Figure 7 as well. Similar surface morphology for DI water also can be observed in another study (Arafat et al., 2023; He et al., 2017). Overall, the adhesive wear mechanism and poorer tribological performance is as expected since the tribo-pairs are of same material and the water on its own is too thin to provide sufficient lubricating film to separate the pure asperities between the pressurized sliding surfaces (Devaraju, 2015).

Furthermore, abrasive wear and oxidation wear are more prevalent in the WBLs with ceramic-based nanoparticles. The abrasive wear can be deduced through the scratches and parallel grooves on the wear surface, whereas the oxidative wear is shown through the black spots on the wear surface (Sharul et al., 2020; Xie et al., 2017). The EDX results of nanolubricants with higher O content than DI water further prove the presence of oxidative wear. Additionally, the presence of the nanoparticles on the worn surface indicated by the EDX results may have helped reduce

adhesive wear by separating the contacting surface, which improves the tribological performance of the formulated WBLs over DI water as well.

Other than nanoparticles, the EDX results also indicate the presence of relatively higher amounts of oxygen and sulfur on the wear surface for MgO WBLs (see Figure 10 middle), suggesting the formation of some form of oxide and sulfide tribofilm. Hence, the tribo-film may be the reason for the better tribological performance of most of the MgO WBLs over DI water. This is because the hard tribo-oxide layer on the surface can prevent the sliding pairs from contacting directly, which discourage adhesion wear and reduce the wear rate (Zhang et al., 2013), whereas sulfide tribo-film possess lower shear strength than metals, creating shearing effect that lower the friction coefficients (Komvopoulos et al., 2003; Liu & Xiong, 2013). However, the reason SiC WBL appears to unable to form such tribofilm may be due to the angular shape of SiC mentioned earlier as well (Zhang et al., 2016).

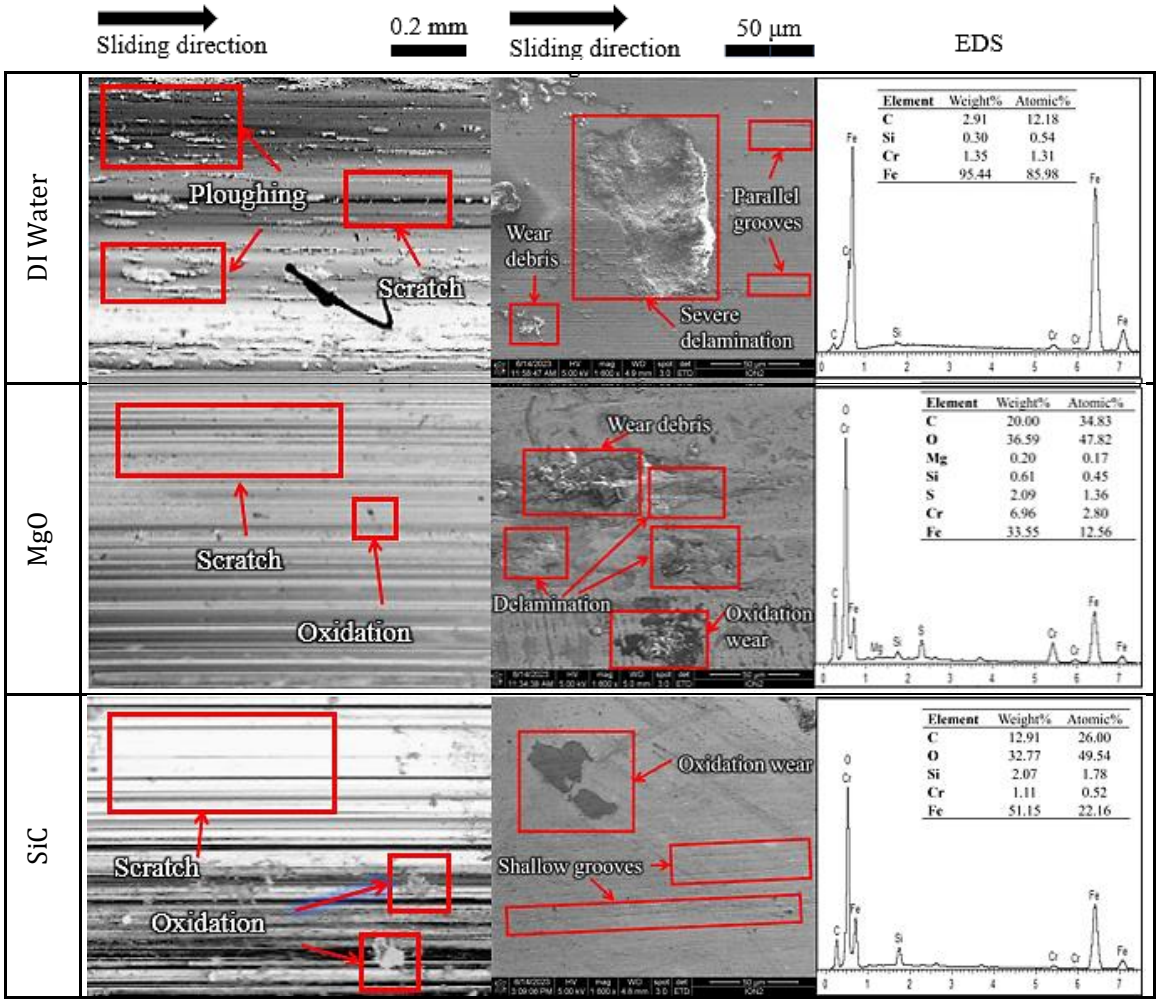

Figure 10: Worn out images of the cylindrical block for different test lubricants. Microscope images (left), FESEM (middle) and EDX results (right).

3.6 Lubrication Mechanisms

Since the TEM micrographs as presented in Figure 4 shows that the MgO nanoparticles are of near-spherical shape, its lubrication mechanism is expected to be mainly bearing effect, where it converts the sliding friction into rolling friction which is lower, while enhancing the friction performance and surface load capacity (Srinivasan et al., 2020). Through initiating bearing effect, the MgO nanoparticles can effectively reduce friction coefficient as well as running-in period as shown in Figure 6 (Syahir & Zulkifli, 2020). Additionally, softer nanoparticles such as MgO may deform and be squeezed into thin films under high load to maintain the lubrication film without damaging the surface as illustrated in Figure 11(a) (Wang et al., 2017).

Similarly, the FESEM-EDS shown in Figure 10 suggest that SiC nanoparticles with near-spherical shape also can act as ball bearing during the tribological process (Wang et al., 2017; Yao et al., 2021). However, the FESEM-EDS depicted in Figure 10 revealed that iron atom may adhere to SiC nanoparticle and limit its rolling motion as illustrated in Figure 11(b). This sliding motion of hard and abrasive SiC nanoparticles will lead to polishing effect, instead of bearing effect (He et al., 2021). In fact, polishing effect is common for nanoparticles with higher hardness, elastic modulus, and compressive strength, such as SiC nanoparticles, which can act as abrasive grains (Han et al., 2022). This creates a smoother surface which can reduce friction and wear, which is the case for SiC WBL.

However, the polishing effect may also have severe effects. Firstly, the nanoparticles can significantly increase and accelerate wear, as evidenced in Figure 8 for the SiC WBL, if the abrasion process persists beyond the initial smoothening of the surface roughness. Secondly, the abrasive action of hard nanoparticles could affect other lubrication mechanism, such as the formation of tribo-films like SiC WBL (Nyholm & Espallargas, 2023). Thirdly, the hard nanoparticles may embed in the comparatively softer surfaces under severe conditions, such as high loads and speed, aggravating two-body abrasive wear (Nyholm & Espallargas, 2023). It is clearly seen that the negative impact of polishing effect is more apparent in the SiC WBL as shown by its larger wear area in Figure 8.

Other than that, nanoparticles can create mending effect by filling up the craters and grooves on the surface, which recover the surface and improve the frictional properties of the surface (He et al., 2017). According to Xie et al. (2017), the filling of valleys between the asperities will occur if the diameter of the spherical particle is less than *Ra* 0.67 μm. Therefore, it may be difficult for nanoparticles of 20-40 nm used in this study to act as a third body material filling in the micro-gaps of the block specimen with *Ra* 0.0363 μm surface roughness. However, it is possible for them to fill in the peaks and valley of the ring specimen with *Ra* 0.6453 μm surface roughness.

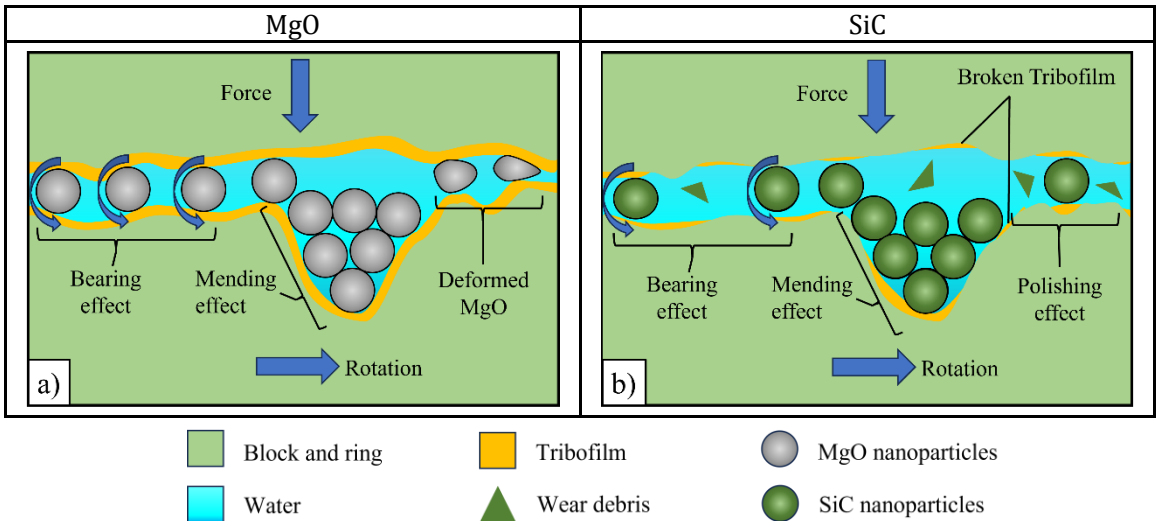

Figure 11: Lubrication mechanism of (a) MgO and (b) SiC WBLs.

CONCLUSIONS

The formulation, development, and evaluation of novel WBLs incorporating ceramic-based nanoparticles MgO and SiC were successfully carried out. Three different WBL formulations were investigated, and their physical, mechanical, and tribological properties were assessed. The addition of nanoparticles to the WBLs enhanced their sedimentation and dispersion stability, particularly with the use of surfactants like PVP. By incorporating glycerol, the viscosity of the WBLs was further increased, as confirmed by rheology and absolute viscosity measurements, resulting in a thicker lubricating agent suitable for optimal tribological performance. Compared to using DI water alone, the formulated WBLs exhibited improved friction, wear, temperature resistance, and lubrication mechanisms. Among the formulated and developed WBLs, the MgO-based WBL showed superior tribological performance in terms of friction, wear, and thermal characteristics. On the other hand, the SiC-based WBL demonstrated exceptional anti-wear properties, mainly attributed to its polishing effect. The outstanding tribological performance of the MgO-based WBL can be attributed to its deformability and bearing effect.

ACKNOWLEDGMENTS

The authors would like to declare that this study and publication were supported by the Ministry of Higher Education under Fundamental Research Grant Scheme (FRGS/1/2022/TK10/UPM/02/9) and the Universiti Putra Malaysia GP-IPM (UPM/GP-IPM/2022/9717500). The authors would like to extend their gratitude to the Department of Mechanical and Manufacturing Engineering, Faculty of Engineering, Universiti Putra Malaysia for their assistance and for making their facilities available at every stage of this research.

REFERENCES

Abe, Y., Sugiura, K., & Mori, K. I. (2020). Ironing limit of aluminium alloy cups with lubricants containing nanoparticles and tool steel die. Procedia Manufacturing, 50, 114–118. https://doi.org/10.1016/j.promfg.2020.08.021

Ahamed, M. M., Basha, S. M. J., & Prasad, B. D. (2020). Comparison of Thermo-Physical and Tribological Characteristics of Nanolubricant. Lecture Notes in Mechanical Engineering, 153–164. https://doi.org/10.1007/978-981-32-9931-3_16

Akilu, S., Sharma, K. V., Baheta, A. T., Azman, M. S. M., & Bhaskoro, P. T. (2016). Temperature Dependent Properties of Silicon Carbide Nanofluid in Binary Mixtures of Glycerol-Ethylene Glycol. Procedia Engineering, 148, 774–778. https://doi.org/10.1016/j.proeng.2016.06.555

Ammarullah, M. I., Hidayat, T., Lamura, M. D. P., & Jamari, J. (2023). Relationship between deformation and running-in wear on hardon-hard bearings from metal, ceramic, and diamond materials for total hip prosthesis. Jurnal Tribologi, 38 (September 2022), 69–81.

Arafat, R., Köhn, C., Jean-Fulcrand, A., Abraham, T., Garnweitner, G., & Herrmann, C. (2023). Physical-chemical properties and tribological characterization of water-glycerine based metal oxide nanofluids. Journal of Materials Research and Technology. https://doi.org/10.1016/j.jmrt.2023.06.073

ASTM International. (2022). Standard Test Method for Ranking Resistance of Materials to Sliding Wear Using Block-on-Ring Wear Test (Patent No. ASTM G77-17). https://www.astm.org/g0077-17r22.html

Awang, M. S. M., Mohd Zulkifli, N. W., Abbas, M. M., Zulkifli, M. S. A., Kalam, M. A., Mohd Yusoff, M. N. A., Ahmad, M. H., & Wan Daud, W. M. A. (2022). Effect of plastic pyrolytic oil and waste cooking biodiesel on tribological properties of palm biodiesel-diesel fuel blends. http://dx.doi.org/10.1108/ILT-08-2021-0338

Chen, W., Zou, C., Li, X., & Li, L. (2017). Experimental investigation of SiC nanofluids for solar distillation system: Stability, optical properties and thermal conductivity with saline water-based fluid. International Journal of Heat and Mass Transfer, 107, 264–270. https://doi.org/10.1016/j.ijheatmasstransfer.2016.11.048

Chu, H. Y., Hsu, W. C., & Lin, J. F. (2010). Scuffing mechanism during oil-lubricated block-on-ring test with diamond nanoparticles as oil additive. Wear, 268(11–12), 1423–1433. https://doi.org/10.1016/j.wear.2010.02.016

Devaraju, A. (2015). A Critical Review on Different Types of Wear of Materials. International Journal of Mechanical Engineering and Technology, 6(11), 77–83.

Ding, Y., Hou, B., Xu, Z., & Fei, L. (2018). Surface modification of calcium carbonate nanoparticles as hydraulic oil additives friction performance research. Functional Materials, 25(3), 584–587.

Hafis, S. M., Ridzuan, M. J. M., Farahana, R. N., Ayob, A., & Syahrullail, S. (2013). Paraffinic mineral oil lubrication for cold forward extrusion: Effect of lubricant quantity and friction. Tribology International, 60, 111-115.

Han, K., Zhang, Y., Song, N., Yu, L., Zhang, P., Zhang, Z., Qian, L., & Zhang, S. (2022). The Current Situation and Future Direction of Nanoparticles Lubricant Additives in China. Lubricants, 10(11), 312. https://doi.org/10.3390/lubricants10110312

He, A., Huang, S., Yun, J. H., Wu, H., Jiang, Z., Stokes, J., Jiao, S., Wang, L., & Huang, H. (2017). Tribological Performance and Lubrication Mechanism of Alumina Nanoparticle Water-Based Suspensions in Ball-on-Three-Plate Testing. Tribology Letters, 65(2). https://doi.org/10.1007/s11249-017-0823-y

He, J., Sun, J., Meng, Y., Pei, Y., & Wu, P. (2021). Synergistic lubrication effect of Al2O3 and MoS2 nanoparticles confined between iron surfaces: a molecular dynamics study. Journal of Materials Science, 56(15), 9227–9241. https://doi.org/10.1007/s10853-021-05889-z

Holmberg, K., & Erdemir, A. (2019). The impact of tribology on energy use and CO2 emission globally and in combustion engine and electric cars. Tribology International, 135, 389–396. https://doi.org/10.1016/j.triboint.2019.03.024

Huang, S., He, A., Yun, J.-H., Xu, X., & Jiang, Z. (2019). Synergistic tribological performance of a water based lubricant using graphene oxide and alumina hybrid nanoparticles as additives. https://ro.uow.edu.au/eispapers1https://ro.uow.edu.au/eispapers1/2404

Komvopoulos, K., Do, V., Yamaguchi, E. S., & Ryason, P. R. (2003). Effect of sulfur- and phosphorus-containing additives and metal deactivator on the tribological properties of boundary-lubricated steel surfaces. Tribology Transactions, 46(3), 315–325. https://doi.org/10.1080/10402000308982632

Liu, R. T., & Xiong, X. (2013). Tribological properties of sulfur-containing high-speed steels at elevated temperature. Transactions of Nonferrous Metals Society of China (English Edition), 23(6), 1674–1680. https://doi.org/10.1016/S1003-6326(13)62647-3

MatWeb. (n.d.). AISI E 52100 Steel. Retrieved February 6, 2023, from https://www.matweb.com/search/datasheet.aspx?matguid=d0b0a51bff894778a97f5b72e7317d85&ckck=1

Morshed, A., Wu, H., & Jiang, Z. (2021). A comprehensive review of water-based nanolubricants. In Lubricants (Vol. 9, Issue 9). MDPI. https://doi.org/10.3390/lubricants9090089

Paijan, L. H., Maleque, A., Adeyemi, B. K., Mamat, M. F., & Hussein, N. I. S. (2023). Influence of ceramic particles size on the incorporation of SiC into stainless steel material using 480 J/mm heat input for tribological applications. Jurnal Tribologi, 37 (April 2022), 15–28.

Qamar, A., Anwar, Z., Ali, H., Shaukat, R., Imran, S., Arshad, A., Ali, H. M., & Korakianitis, T. (2022). Preparation and dispersion stability of aqueous metal oxide nanofluids for potential heat transfer applications: a review of experimental studies. In Journal of Thermal Analysis and Calorimetry (Vol. 147, Issue 1, pp. 23–46). Springer Science and Business Media B.V. https://doi.org/10.1007/s10973-020-10372-z

Rahman, M. H., Warneke, H., Webbert, H., Rodriguez, J., Austin, E., Tokunaga, K., Rajak, D. K., & Menezes, P. L. (2021). Water-based lubricants: Development, properties, and performances. In Lubricants (Vol. 9, Issue 8). MDPI AG. https://doi.org/10.3390/lubricants9080073

Sharul, M., Awang, N., Wahidah, N., Zulkifli, M., Abbass, M. M., Zulkifli, S. A., Ashraf, M. N., Yusoff, M., Ahmad, M. H., Ashri, W. M., & Daud, W. (2020). Effect of blending local plastic pyrolytic oil with diesel fuel on lubricity. Jurnal Tribologi, 27 (November), 143–157.

Sidh, K. N., Jangra, D., & Hirani, H. (2023). An Experimental Investigation of the Tribological Performance and Dispersibility of 2D Nanoparticles as Oil Additives. Lubricants, 11(4). https://doi.org/10.3390/lubricants11040179

Seidel, B., & Meyer, D. (2019). Investigation of the Influence of Aging on the Lubricity of Metalworking Fluids by Means of Design of Experiment. Lubricants, 7(11), 94. https://doi.org/10.3390/lubricants7110094.

Sharuddin, M. H. B., Sulaiman, M. H., Kamaruddin, S., Dahnel, A. H., Abd Halim, N. F. H., Ridzuan, M. J. M., & Abdul-Rani, A. M. (2023). Properties and tribological evaluation of graphene and fullerene nanoparticles as additives in oil lubrication. Proceedings of the Institution of Mechanical Engineers, Part J: Journal of Engineering Tribology, 13506501231175540. https://doi.org/10.1177/13506501231175540

Singh, Y., Badhotiya, G. K., Gwalwanshi, M., Negi, P., & Bist, A. (2021). Magnesium oxide (MgO) as an additive to the neem oil for efficient lubrication. Materials Today: Proceedings, 46, 10478–10481. https://doi.org/10.1016/j.matpr.2020.12.1181

Smazalová, E., Houdková, Š., & Švantner, M. (2014). Tribological Effects of Discontinuous Block-on-Ring Test. https://www.confer.cz/metal/2014/3136-tribological-effects-of-discontinuous-block-on-ring-test

Srinivasan, N., Rajenthirakumar, D., Sridhar, R., & Amutha, P. (2020). Tribomechanical performance of MgO–ZnO nanoparticles as lubricating additives in the microextrusion process. Proceedings of the Institution of Mechanical Engineers, Part C: Journal of Mechanical Engineering Science, 234(22), 4543–4553. https://doi.org/10.1177/0954406220922859

Sulaiman, M. H., Farahana, R. N., Bienk, K., Nielsen, C. V., & Bay, N. (2019). Effects of DLC/TiAlN-coated die on friction and wear in sheet-metal forming under dry and oil-lubricated conditions: Experimental and numerical studies. Wear, 438, 203040. https://doi.org/10.1016/j.wear.2019.203040

Syahir, M., & Zulkifli, A. Bin. (2020). Tribological Investigation of Ionic Liquids as Bio-Based Lubricant Additive For Engine Oil Formulation. Tribology Transactions

Wang, J., Hu, W., & Li, J. (2021). Lubrication and anti-rust properties of jeffamine-triazole derivative as water-based lubricant additive. Coatings, 11(6). https://doi.org/10.3390/coatings11060679

Wang, Y., Li, C., Zhang, Y., Yang, M., Zhang, X., Zhang, N., & Dai, J. (2017). Experimental evaluation on tribological performance of the wheel/workpiece interface in minimum quantity lubrication grinding with different concentrations of Al2O3 nanofluids. Journal of Cleaner Production, 142, 3571–3583. https://doi.org/10.1016/j.jclepro.2016.10.110

Wu, H., Wang, L., Johnson, B., Yang, S., Zhang, J., & Dong, G. (2018). Investigation on the lubrication advantages of MoS2 nanosheets compared with ZDDP using block-on-ring tests. Wear, 394–395, 40–49. https://doi.org/10.1016/j.wear.2017.10.003

Xie, H., Jiang, B., Dai, J., Peng, C., Li, C., Li, Q., & Pan, F. (2018). Tribological behaviors of graphene and graphene oxide as water-based lubricant additives for magnesium alloy/steel contacts. Materials, 11(2). https://doi.org/10.3390/ma11020206

Xie, H., Jiang, B., Hu, X., Peng, C., Guo, H., & Pan, F. (2017). Synergistic effect of MoS2 and SiO2 nanoparticles as lubricant additives for magnesium alloy–steel contacts. Nanomaterials, 7(7). https://doi.org/10.3390/nano7070154

Yang, Y., Oztekin, A., Neti, S., & Mohapatra, S. (2012). Particle agglomeration and properties of nanofluids. Journal of Nanoparticle Research, 14(5). https://doi.org/10.1007/s11051-012-0852-2

Yao, C., Chen, D., Xu, K., Zheng, Z., Wang, Q., & Liu, Y. (2021). Study on nano silicon carbide water-based cutting fluid in polysilicon cutting. Materials Science in Semiconductor Processing, 123. https://doi.org/10.1016/j.mssp.2020.105512

Zahedi, E., Woerz, C., Reichardt, G., Umlauf, G., Liewald, M., Barz, J., Weber, R., Foerster, D. J., & Graf, T. (2019). Lubricant-free deep drawing using CO2 and N2 as volatile media injected through laser-drilled microholes. Manufacturing Review, 6. https://doi.org/10.1051/mfreview/2019011

Zhang, Q. Y., Chen, K. M., Wang, L., Cui, X. H., & Wang, S. Q. (2013). Characteristics of oxidative wear and oxidative mildwear. Tribology International, 61, 214–223. https://doi.org/10.1016/j.triboint.2013.01.003

Zhang, X., Li, C., Zhang, Y., Jia, D., Li, B., Wang, Y., Yang, M., Hou, Y., & Zhang, X. (2016). Performances of Al2O3/SiC hybrid nanofluids in minimum-quantity lubrication grinding. International Journal of Advanced Manufacturing Technology, 86(9–12), 3427–3441. https://doi.org/10.1007/s00170-016-8453-3

Zhou, M., Jia, F., Yan, J., Wu, H., & Jiang, Z. (2022). Lubrication Performance and Mechanism of Water-Based TiO2 Nanolubricants in Micro Deep Drawing of Pure Titanium Foils. Lubricants, 10(11), 292. https://doi.org/10.3390/lubricants10110292